scientific reports

Check for updates

OPEN

Thermodynamic assessment of tri-reforming of methane with optimization of operating conditions to achieve suitable syngas for methanol production

Amin Alamdari✉, Mohammad Javad Azarhoosh✉ & Abbas Aghaeinejad-Meybodi

The present study consists of two parts. In the first part, a thermodynamic assessment of the reactions involved in the tri-reforming of methane (TRM) to syngas was conducted using a stoichiometric approach by simultaneously solving a system of nonlinear equilibrium equations. Using the results, the effects of operational variables, including temperature, pressure, and the molar ratios of H_2O, CO_2, and O_2 to CH_4, were investigated on reactant conversions, product yields, and the H_2/CO ratio. The results revealed that while increasing temperature promotes CH_4 and CO_2 conversions, H_2O conversion exhibits a non-monotonic trend due to the competition between reforming and the reverse water-gas shift (RWGS) reaction. Higher temperatures and lower pressures generally enhance the yields of H_2 and CO, though the H_2/CO ratio decreases as temperature rises. Furthermore, increasing the CO_2 feed ratios reduces the H_2/CO ratio, whereas increasing the H_2O ratio effectively enriches the syngas with hydrogen. In the second part, a Genetic Algorithm (GA) was employed to identify optimal operating conditions for producing syngas with a target H_2/CO ratio of 2.0, suitable for methanol synthesis, subject to CH_4 and CO_2 conversion constraints exceeding 90%. The optimal conditions were identified as: Temperature = 989 °C, Pressure = 1.0 bar, and a feed ratio of CH_4:H_2O: CO_2:O_2 = 1:0.61:0.30:0.10. Under these optimized parameters, a CH_4 conversion of 99.8% and a CO_2 conversion of 90.0% were achieved, yielding a syngas ratio of 1.99. These results are fully consistent with industrial requirements for methanol synthesis and align with the parametric sensitivity trends established in the thermodynamic analysis.

Keywords Tri-reforming of methane, Syngas, Methanol production, Thermodynamic assessment, Optimization, Genetic algorithm

Abbreviations

DMR	Dry methane reforming
GA	Genetic algorithm
GFEM	Gibbs Free Energy Minimization
POX	Partial oxidation of methane
SMR	Steam methane reforming
WGSR	Water-Gas shift reaction
RWGS	Reverse water-gas shift reaction

List of symbols

$C_{p_i}(kJ.mol^{-1}.K^{-1})$	Specific heat capacity of component *i* at constant pressure
K_a	Equilibrium constant based on activity
K_p	Equilibrium constant based on partial pressure
K_y	Equilibrium constant based on mole fraction
n_i^{eq}	Number of moles of component *i* at equilibrium
n_i^0	Initial number of moles of component *i*

Department of Chemical Engineering, Faculty of Engineering, Urmia University, Urmia, Iran. ✉email: a.alamdari@urmia.ac.ir; mj.azarhoosh@urmia.ac.ir

n_{tot}	Total number of moles at equilibrium
$P_{tot}\,(bar)$	Total system pressure
$R(Pa.m^3.mol^{-1}.K^{-1})$	Universal gas constant
$T\,(K)$	Absolute reaction temperature
$X_i\,(\%)$	Equilibrium conversion of reactants (CH_4, H_2O, CO_2)
$Y_i\,(\%)$	Molar yield of products (H_2 and CO)
$\Delta C_p(kJ.mol^{-1}.K^{-1})$	Change in the specific heat capacity of the reaction at temperature T
$\Delta G\,(T)\,(kJ.mol^{-1})$	Change in Gibbs free energy of the reaction at temperature T
$\Delta H_r\,(T)\,(kJ.mol^{-1})$	Change in reaction enthalpy at temperature T
$\Delta H^o_{r_{298}}(kJ.mol^{-1})$	Standard reaction enthalpy at 298 K
Δn	Difference in the stoichiometric coefficients between products and reactants
$\Delta S\,(T)\,(kJ.mol^{-1}.K^{-1})s$	Change in reaction entropy at temperature T

The tri-reforming of methane (TRM) process is an advanced technology for producing syngas (a mixture of hydrogen (H_2) and carbon monoxide (CO)) from methane (CH_4)[1]. This process combines three main reforming reactions—steam methane reforming (SMR), dry methane reforming (DMR), and partial oxidation of methane (POX)—into a single integrated system. The intelligent integration of these three reactions in one reactor or system to overcome the challenges of each individually and achieve operational efficiency has made this process highly attractive[2,3]. One of the advantages of TRM is its ability to produce syngas with a desired H_2/CO ratio (typically between 1.5 and 2.5) for various applications[4]. Furthermore, the heat generated from POX supplies energy for the endothermic SMR and DMR reactions, significantly reducing the need for external heating and improving the overall energy efficiency of the process[5]. Additionally, coke formation and subsequent catalyst deactivation are greatly minimized in this process. The presence of steam (H_2O) and carbon dioxide (CO_2) helps prevent coke deposition on the catalyst. Moreover, the endothermic nature of SMR and DMR reactions reduces local temperatures, further suppressing coking[6,7]. Another advantage is the consumption of greenhouse gas CO_2, which can be sourced from various outlets such as associated gas, flue gases, or even the atmosphere, as a useful feedstock. The process also allows the use of diverse CH_4 sources, such as natural gas and biogas, and enables the adjustment of reactant ratios to achieve the desired product[8,9].

In other words, the TRM has emerged as a promising and versatile technology for syngas production, primarily due to its unique ability to integrate three distinct reactions: SMR, DMR, and POX within a single catalytic reactor. The fundamental advantage of this process lies in its synergistic thermal management. While SMR and DMR are highly endothermic and require significant external energy, the exothermic nature of POX provides in-situ heat, potentially leading to an autothermal operation. This drastically reduces the energy intensity of the process and improves the overall thermal efficiency, making it more economically viable for large-scale applications[10,11].

From a chemical perspective, TRM offers unparalleled flexibility in tuning the H_2/CO molar ratio. For industrial processes such as Methanol synthesis and Fischer-Tropsch synthesis, a specific ratio (typically around 2.0) is required. Traditional SMR often yields a ratio higher than 3.0, while DMR results in a ratio close to 1.0. By carefully adjusting the feed composition (CH_4, CO_2, H_2O, and O_2), TRM can precisely target the desired syngas quality while simultaneously utilizing CO_2, a major greenhouse gas, as a reactant[12].

Regarding the catalytic systems, significant research has been dedicated to developing materials that can withstand the harsh, high-temperature environment of TRM. Nickel-based catalysts supported on metal oxides such as Al_2O_3, MgO, ZrO_2, and CeO_2 are widely used due to their low cost and high initial activity. However, they are prone to deactivation via carbon deposition (coking) and thermal sintering[13,14]. Recent literature has focused on enhancing these catalysts by adding promoters like alkaline earth metals or noble metals (e.g., Ru, Rh, Pt) to improve oxygen mobility and suppress carbon formation. For instance, the use of CeO_2 as a support or promoter has shown remarkable results in oxygen storage capacity, which facilitates the gasification of carbonaceous species. Operating temperatures for these systems typically range between 700 °C and 950 °C at atmospheric or elevated pressures, depending on the downstream integration requirements[15,16].

Thermodynamic evaluation of the TRM reactions provides the scientific basis for process design and is crucial for optimizing performance, predicting system behavior, and preventing operational issues. This assessment is used to predict reaction feasibility and chemical equilibrium, study the effects of temperature, pressure, and reactant ratios on conversion rates and syngas yield, optimize the H_2/CO ratio in syngas, reduce coke production, and predict thermal equilibrium conditions to achieve autothermal operation[17–20]. A few thermodynamic studies have been conducted on the TRM process. Zhang et al. conducted a thermodynamic analysis of the TRM process using the Gibbs free energy minimization method and then investigated the effect of operating variables on the product distribution[17]. Szczygieł et al.[18] evaluated the TRM and DRM processes, and Chein and Hsu[19] evaluated the TRM and carbon gasification (CG) processes from a thermodynamic perspective. Furthermore, in a similar study, Okonkwo et al. evaluated the thermodynamics of tri-reforming of oxyfuel combustion exhaust gas[21].

Several studies have focused on the optimization of the Tri-Reforming of Methane (TRM) process using various techniques. Table 1 shows a detailed comparison of optimization Studies in TRM.

Problem statement and innovations of this study

The present study consists of two parts. In the first part, a thermodynamic analysis of the TRM is conducted. The equilibrium composition of components is calculated under various operating conditions and feed ratios. Using these results, the effects of temperature, pressure, and the ratios of steam to methane (H_2O/CH_4), carbon dioxide to methane (CO_2/CH_4), and oxygen to methane (O_2/CH_4) in the feed on the CH_4, CO_2, and H_2O conversion, as well as the H_2 and CO yield and their ratio in the produced syngas, are investigated.

Reference No.	Optimization Technique	Objective Functions	Variables	Method	Constraints
[8]	Multi-Objective Genetic Algorithm (NSGA-II)	Maximizing CH_4 conversion, Minimizing CO_2 emissions, and adjusting H_2/CO ratio	Temperature, Pressure, and O_2/CH_4, H_2O/CH_4, CO_2/CH_4 ratios.	Gibbs free energy minimization (GFEM)	Bound constraints on operating variables
[18]	Response Surface Methodology (RSM) and Statistical Analysis.	Yield of syngas components and thermal efficiency	Feed molar ratios (H_2O, CO_2, O_2 to methane)	Thermodynamic equilibrium based on GFEM	Range of feed compositions
[22]	Direct Search/Kinetic-based Optimization	Maximizing Methanol production yield in an integrated TRM-Methanol loop	Reactor dimensions, feed temperature, and pressure	Kinetic modeling and mass/energy balances	Maximum allowable reactor temperature to prevent catalyst sintering
[9]	Parametric sensitivity and side-feeding policy optimization.	CO_2 conversion and H_2/CO ratio control	Injection points for O_2, H_2O, or CO_2	Thermodynamic and kinetic simulation	Autothermal operation conditions

Table 1. Detailed Comparison of Optimization Studies in TRM.

Another key advantage of the TRM process is its ability to adjust the H_2/CO ratio in the syngas produced. Different H_2/CO ratios are crucial for various chemical and industrial processes. Theoretically, syngas with an H_2/CO ratio of 2:1 is suitable for methanol production. Methanol production from syngas is one of the most fundamental and important processes in the petrochemical and chemical industries, holding significant economic, industrial, and environmental importance[22,23]. Therefore, this study calculates the optimal operating conditions for producing syngas suitable for methanol production using a genetic algorithm (GA) optimization approach.

The novelty of the present study is twofold:

Methodological novelty (stoichiometric vs. non-stoichiometric)

Most existing studies rely on the Gibbs Free Energy Minimization (GFEM), which is a non-stoichiometric approach. In this work, a direct system of nonlinear equilibrium constant equations (stoichiometric) is utilized. When integrated into a GA requiring thousands of iterations, this stoichiometric approach ensures higher computational stability and transparency. It guarantees that the optimization path strictly follows the specific reaction network (SMR, DMR, WGS), avoiding potential convergence issues or "black-box" numerical errors often encountered in GFEM-based iterative loops. Unlike GFEM, the stoichiometric approach allows for a direct coupling of specific reaction extents, providing deeper mechanistic insights into how individual reactions like RWGS or DMR respond to perturbations in feed composition.

Optimization constraint novelty

Unlike previous studies that often optimize for a "general maximum yield," the GA used in this study specifically designed to hit an exact industrial target (H_2/CO = 2) while simultaneously satisfying strict inequality constraints (> 90% conversion) for both methane and carbon dioxide. This makes the results more applicable to the specific requirements of a downstream methanol synthesis unit.

Reaction network

The TRM process is based on three simultaneous main reactions, which are[24,25]:

- SMR:

$$CH_4 + H_2O \rightleftharpoons CO + 3H_2 \Delta H^o_{r_{298}} = 206 kJ.mol^{-1} \quad (1)$$

- DMR:

$$CH_4 + CO_2 \rightleftharpoons 2CO + 2H_2 \Delta H^o_{r_{298}} = 247 kJ.mol^{-1} \quad (2)$$

- POX:

$$CH_4 + 0.5O_2 \rightleftharpoons CO + 2H_2 \Delta H^o_{r_{298}} = -36 kJ.mol^{-1} \quad (3)$$

In addition to the three main reactions, the following reactions also occur in the process reactor[24,25]:

- CH_4 full combustion:

$$CH_4 + 2O_2 \rightleftharpoons CO_2 + 2H_2O \Delta H^o_{r_{298}} = -802 kJ.mol^{-1} \quad (4)$$

- Water-gas shift reaction (WGSR):

$$CO + H_2O \rightleftharpoons CO_2 + H_2 \Delta H^o_{r_{298}} = -41 kJ.mol^{-1} \quad (5)$$

Furthermore, reactions such as CH_4 decomposition, Boudouard reaction, and Boggs reaction may occur, leading to coke deposition on the catalyst surface and subsequently reducing its activity. These reactions are considered

in calculations related to catalyst activity coefficients in the simulation of TRM reactors. The thermodynamic evaluation in this study was performed using the Equilibrium Constant Method (a stoichiometric approach). In a stoichiometric framework, incorporating heterogeneous phases (solid carbon) introduces significant mathematical challenges, such as phase-boundary discontinuities. This often leads to numerical instability or convergence issues when solving the non-linear system of equations across a wide temperature range. Also, by focusing on the 700–1000 °C range in this study and in the presence of H_2O and O_2, the thermodynamic driving force for the Boudouard reaction and methane decomposition is effectively suppressed. So, the gas-phase equilibrium assumption becomes physically sound and highly reliable and the Boudouard reaction and other carbon deposition reactions are not included in the thermodynamic analysis[26,27].

To assess the feasibility of the aforementioned reactions and determine whether they are spontaneous or non-spontaneous at different temperatures, the Gibbs free energy of the reactions must be calculated. The Gibbs free energy of a reaction is a criterion that determines the spontaneity and direction of a chemical reaction under varying temperature conditions and constant pressure. It depends on both the enthalpy change and entropy change of the reaction and is calculated using the Gibbs-Helmholtz equation[21]:

$$\Delta G\left(T\right) = \Delta H_r\left(T\right) - T\Delta S\left(T\right) \tag{6}$$

The changes in enthalpy and entropy of reactions at different temperatures are obtained using the following relationships[21]:

$$\Delta H_r\left(T\right) = \Delta H^o_{r_{298}} + \int_{298}^{T} \Delta C_p dT \tag{7}$$

$$\Delta S\left(T\right) = \Delta S^o_{298} + \int_{298}^{T} \frac{\Delta C_p}{T} dT \tag{8}$$

$$\Delta C_p = \sum C_{pProducts} - \sum C_{pReactants} \tag{9}$$

Figure 1 shows the changes in the Gibbs free energy of TRM reactions as a function of temperature in the range of 0 to 1500 °C. As observed, within the studied temperature range, the POX and CH_4 full combustion reactions exhibit negative Gibbs free energy values, indicating that they are spontaneous.

The SMR and DMR reactions become spontaneous at temperatures above 622 °C and 646 °C, respectively. Below these temperatures, they are non-spontaneous and proceed in the reverse direction. However, the WGS reaction shows an opposite trend. This reaction is spontaneous at temperatures below 868 °C, while at higher temperatures, the reverse water-gas shift (RWGS) reaction becomes spontaneous. These findings are highly valuable for analyzing the effect of temperature on the equilibrium composition of various components[17,28].

The equilibrium constants of the TRM reactions can be calculated using the following relation:

$$K_a = e^{\left(\frac{-\Delta G(T)}{RT}\right)} \tag{10}$$

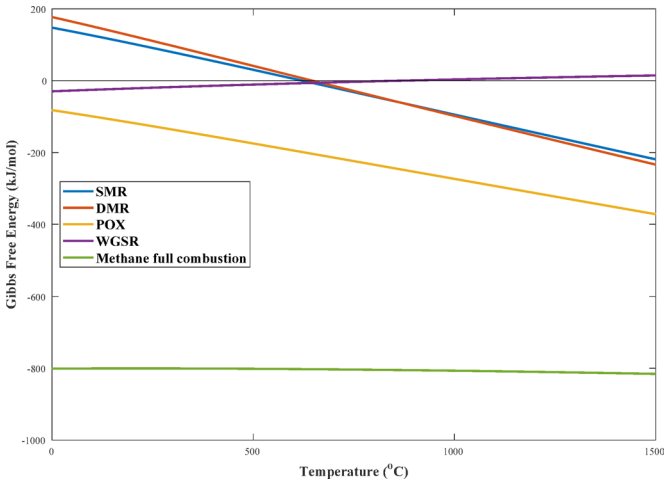

Fig. 1. Plot of Gibbs free energy changes as a function of temperature for TRM reactions.

In the above relation, the equilibrium constant is expressed in terms of the activity (a) of the reaction components. Assuming the reaction components behave as ideal gases and partial pressures are measured in bar, the activity-based equilibrium constant can be considered equivalent to the equilibrium constant expressed in terms of partial pressures (KP)[29]. Figure 2 shows the variations of the equilibrium constants for the reactions under study as a function of temperature. The values of the equilibrium constants are used to calculate the equilibrium composition of various components in the process.

The equilibrium constant in terms of mole fractions of the reaction components (Ky) is calculated according to the following relation[29]:

$$K_y = K_p {P_{tot}}^{-\Delta n} \tag{11}$$

Thermodynamic evaluation of the process

Two methods are commonly used to calculate the equilibrium mole fractions of components in a set of reversible reactions: the reaction equilibrium constant and the Gibbs free energy minimization methods[30]. The Gibbs free energy minimization method is a powerful tool for calculating chemical equilibrium and is preferred for multi-reaction systems with numerous reaction components. However, this method has limitations, including computational complexity, a strong dependence on thermodynamic data, the need to define atomic constraints, and convergence issues in minimization (e.g., divergence due to poor initial guesses or convergence to incorrect local minima)[31].

In the reaction equilibrium constant method used in this study, equilibrium concentrations are determined using the reaction equilibrium constant relation. This method is preferred for single and simple reactions or multiple reactions when the reaction network is known, and the number of unknowns (equilibrium mole fractions of reaction components) equals the number of equations[32].

As observed in Figs. 1 and 2, the POX and CH_4 full combustion reactions exhibit negative Gibbs free energy and very large equilibrium constants within the operational temperature range. Therefore, these reactions can be considered irreversible, and the equilibrium constant relation need not be written for them. Additionally, Under the conditions studied, where the oxygen-to-methane ratio (O_2/CH_4) is kept significantly below the stoichiometric requirement for complete combustion, oxygen acts as the limiting reactant. Therefore, at the thermodynamic equilibrium of the TRM process, it can be concluded that oxygen is virtually entirely consumed, and its equilibrium concentration is assumed to be zero for the purpose of the stoichiometric calculations.

Among the three remaining reactions—SMR, DMR, and WGS —only two are independent. This is because the DMR reaction can be derived from the combination of SMR and the RWGS reactions. Thus, the equilibrium constant equation needs to be written for two of these three reactions.

Apart from the equilibrium mole fraction of oxygen, which is known (zero), the equilibrium mole fractions of the other five components (CH_4, H_2O, CO_2, CO, and H_2) are unknown. Solving for these requires the simultaneous solution of five equations:

- Elemental mass balance for carbon (C):

$$n_{C_{total}} = n^0_{CH_4} + n^0_{CO_2} = {n_{CH_4}}^{eq} + {n_{CO_2}}^{eq} + {n_{CO}}^{eq} \tag{12}$$

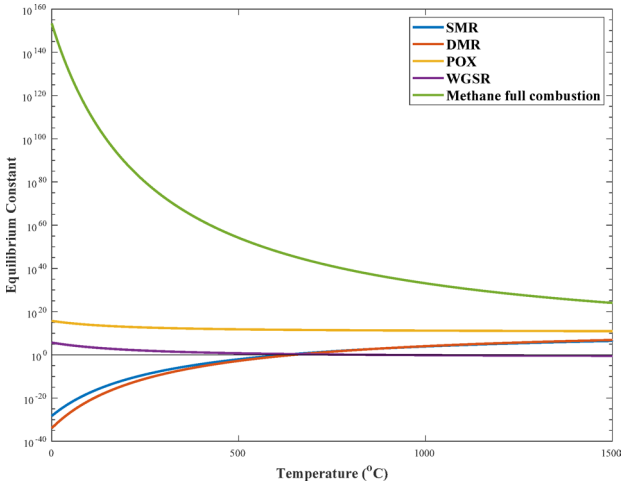

Fig. 2. Plot of equilibrium constant variations as a function of temperature for TRM reactions.

- Elemental mass balance for oxygen (O):

$$n_{O_{total}} = n^0_{H_2O} + 2n^0_{CO_2} + 2n^0_{O_2} = {n_{H_2O}}^{eq} + 2{n_{CO_2}}^{eq} + {n_{CO}}^{eq} \tag{13}$$

- Elemental mass balance for hydrogen (H):

$$n_{H_{total}} = 4n^0_{CH_4} + 2n^0_{H_2O} = 4{n_{CH_4}}^{eq} + 2{n_{H_2O}}^{eq} + 2{n_{H_2}}^{eq} \tag{14}$$

The above elemental balance equations illustrate the conservation of Carbon (C), Hydrogen (H), and Oxygen (O) atoms between the feed and the equilibrium products.

- Equilibrium constant equation for SMR:

$$K_{y_{SMR}} = \frac{n_{CO}{n_{H_2}}^3}{n_{CH_4}n_{H_2O}} \times \left(\frac{1}{n_{tot}}\right)^2 \tag{15}$$

- Equilibrium constant equation for DMR:

$$K_{y_{DR}} = \frac{{n_{CO}}^2{n_{H_2}}^2}{n_{CH_4}n_{CO_2}} \times \left(\frac{1}{n_{tot}}\right)^2 \tag{16}$$

The system of nonlinear equations described above is solved using coding in MATLAB R2024b software with the *fsolve* command. This numerical method is used to find roots of the nonlinear equations by iteratively optimizing initial guesses until convergence is achieved.

Optimization using a GA

A GA is an intelligent optimization and search technique inspired by the principles of natural evolution and genetics. This algorithm is employed to identify optimal or near-optimal solutions for complex, multi-faceted problems[33,34].

In this method, an initial population is first generated randomly. Each individual within the population consists of chromosomes representing the key process variables: temperature, pressure, and the molar ratios of H_2O/CH_4, CO_2/CH_4, and O_2/CH_4 in the feed stream. The fitness function of all individuals in the population is evaluated using the thermodynamic assessment code described in the previous section. In this study, the fitness function is defined as the absolute difference between the hydrogen-to-carbon monoxide (H_2/CO) ratio in the produced syngas and the target value of 2. The objective of the optimization is to minimize this fitness function.

Subsequently, a select percentage of the population is chosen as parents via the Tournament selection method. The crossover operator is then applied to these parents to generate offspring. This study utilizes an Arithmetic crossover technique. Following this, the mutation operator is applied to a subset of the population. For this purpose, the Gaussian method was selected as the mutation operator.

The entire population, comprising the initial individuals, their offspring, and the mutated individuals, is then ranked based on their fitness values. A lower fitness value corresponds to a higher rank. The top-ranked individuals, equal in number to the initial population size (100 individuals in this study), are selected to form the next generation.

This iterative cycle continues until the termination criterion, which is a maximum of 200 generations in this study, is met. Figure 3 illustrates the flowchart of the GA implemented in this work. The optimization was conducted using the GA, with code developed in MATLAB R2024b[11,35,36].

Table 2 summarizes the parameters employed in the GA for the optimization process[37].

Thermodynamic evaluation results

Effect of temperature investigation

Figure 4 illustrates the effect of temperature on the equilibrium conversion of reactants (CH_4, H_2O, and CO_2), the molar yield of products (H_2 and CO), and the equilibrium H_2/CO molar ratio.

The equilibrium conversion of reactants and the molar yield of products are obtained through the following relationships:

$$X_i\,(\%) = \frac{{n_i}^0 - n_i}{{n_i}^0} \times 100 \tag{17}$$

$$Y_{H_2}\,(\%) = \frac{{n_{H_2}}^{eq}}{2n^0_{CH_4} + n^0_{H_2O}} \times 100 \tag{18}$$

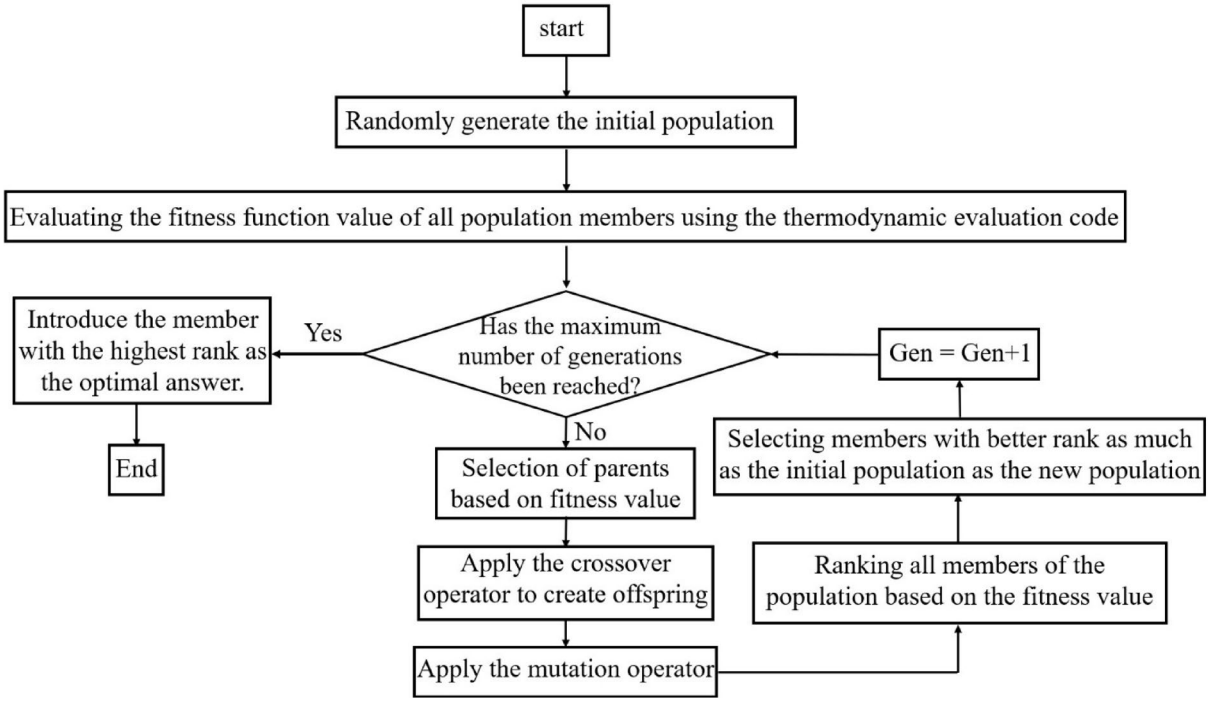

Fig. 3. Flowchart of the GA implemented in the present study.

Parameter	Value/Method
Population Size	100
Number of Generations	200
Parent Selection Method	Tournament
Crossover Method	Arithmetic
Crossover Percentage	70%
Mutation Method	Gaussian
Mutation Percentage	30%

Table 2. Parameters of the GA employed in the present study.

$$Y_{CO}\,(\%) = \frac{{n_{CO}}^{eq}}{n^0_{CH_4} + n^0_{CO_2}} \times 100 \tag{19}$$

As observed in Fig. 4a, the equilibrium CH_4 conversion increases from 78% at 700 °C to 100% at 1000 °C. This behavior can be attributed to the reaction pathways illustrated in Fig. 1. At temperatures above 700 °C, CH_4 is consumed in the CH_4 full combustion, POX, SMR, and DMR reactions, and its consumption rate increases with increasing temperature. CO_2 also shows a similar trend to CH_4, with the conversion increasing from 55% at 700 °C to 86% at 1000 °C. In the temperature range of 700 to 868 °C, CO_2 is produced in two reactions: WGS and CH_4 full combustion, and consumed in the DMR reaction. Given the positive conversion, it can be concluded that the consumption rate is higher. However, at temperatures above 868 °C, the WGS reaction proceeds in the reverse direction, and CO_2 is consumed in two reactions: DMR and RWGS.

For H_2O, the conversion with respect to temperature reaches a maximum at 868 °C. This is because at temperatures lower than 868 °C, H_2O is consumed in the WGS and SMR reactions, and conversion increases with increasing temperature. However, at temperatures higher than that, H_2O is produced in the RWGS reaction, and conversion decreases with temperature.

As illustrated in Fig. 4b, the yield of H_2 and CO increases with temperature. This is attributed to the fact that, syngas (H_2 and CO) is generated via all three main processes: POX, SMR, and DMR. However, it is observed that the yield of CO at temperatures above 868 °C exceeds the yield of H_2. This is because at temperatures below 868 °C, part of the CO produced is converted to H_2 in the WGS reaction. Still, at temperatures above that, the process is reversed.

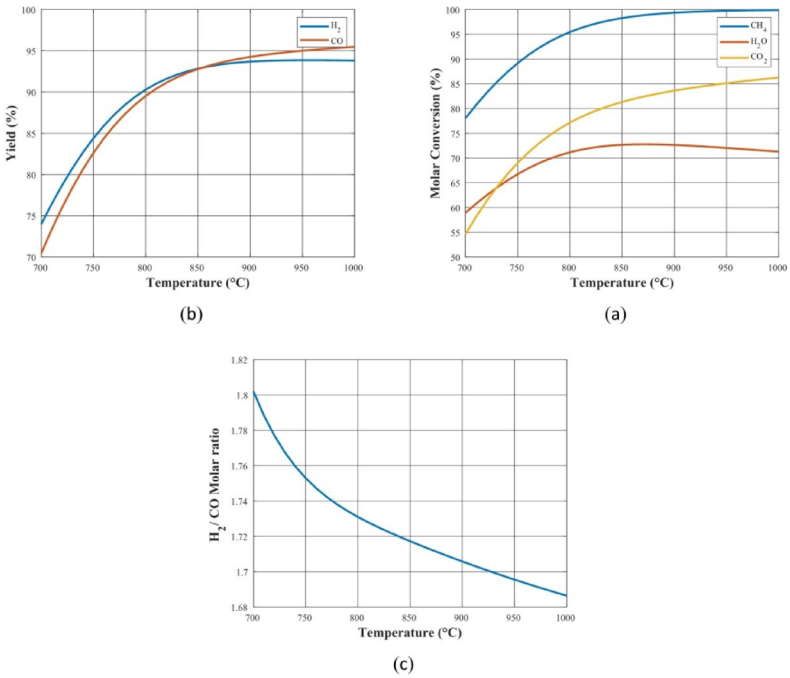

Fig. 4. Plots of **(a)** variations in the equilibrium conversion of reactants, **(b)** molar yield of products, and **(c)** H_2/CO equilibrium molar ratio as a function of temperature at a pressure of 1 bar and a molar feed ratio of CH_4:H_2O: CO_2:O_2 = 1:0.54:0.48:0.1.

Furthermore, as shown in Fig. 4c, the H_2/CO ratio decreases from 1.80 at 700 °C to 1.69 at 1000 °C. This decline occurs because, at lower temperatures, a fraction of the CO produced is converted to H_2 via the WGS reaction, thereby increasing the H_2/CO ratio. At higher temperatures, the WGS reaction equilibrium shifts toward reactants, reducing its influence and resulting in a lower ratio.

Investigation of pressure effect

In this study, the pressure was investigated in the range of 1 to 10 bar. While atmospheric pressure (1 bar) is thermodynamically optimal for methane conversion, the range was extended to 10 bar to assess the process under industrially relevant conditions where downstream integration and reactor volume minimization are critical[27]. Figure 5 illustrates the influence of pressure within the temperature range of 700 to 1000 °C on the conversion of reactants, the yield of products, and the H_2/CO ratio in the produced syngas. As observed, increasing the pressure leads to a decrease in the conversion of CH_4, H_2O, and CO_2, as well as a reduction in the yields of H_2 and CO.

This phenomenon can be explained by Le Chatelier's principle. An increase in system pressure shifts the reaction equilibrium in the direction that counteracts this change by reducing the pressure. Since the SMR and DMR reactions involve an increase in the total number of gaseous moles ($\Delta n_g > 0$), the reverse reaction pathway is favored at higher pressures to reduce the number of moles and, consequently, the pressure. Therefore, elevated pressure promotes the reverse reforming reactions, resulting in lower reactant conversion and a decrease in syngas yield.

However, the results indicate that the conversion of oxygen remains unchanged with varying pressure; oxygen is completely consumed across all pressure levels. This is because, within the studied temperature range, the CH_4 full combustion and POX reactions can be considered irreversible.

The influence of operating pressure on the H_2/CO ratio exhibits a dual and temperature-dependent behavior, as illustrated in Fig. 5f. At lower temperature regimes, an increase in pressure tends to slightly enhance or stabilize the H_2/CO ratio, as the system's equilibrium is heavily influenced by the WGS reactor and methanol-precursor kinetics. However, as the temperature increases, a reversal in this trend occurs. At elevated temperatures, increasing the pressure leads to a reduction in the H_2/CO ratio. This phenomenon can be explained by the Le Chatelier's principle acting on the reforming reactions (SMR and DMR), which involve an increase in the total number of moles. High pressure suppresses these reactions, but its inhibitory effect is more pronounced on the SMR pathway compared to the DMR and RWGS reactions at specific thermal conditions. This conflict between pressure-driven mole reduction and temperature-driven reaction kinetics results in an 'inversion point' where the pressure's impact on syngas quality reverses. Consequently, selecting an optimal pressure is vital, as it must balance the kinetic requirement for high pressure with the thermodynamic necessity of maintaining a H_2/CO ratio near 2.0.

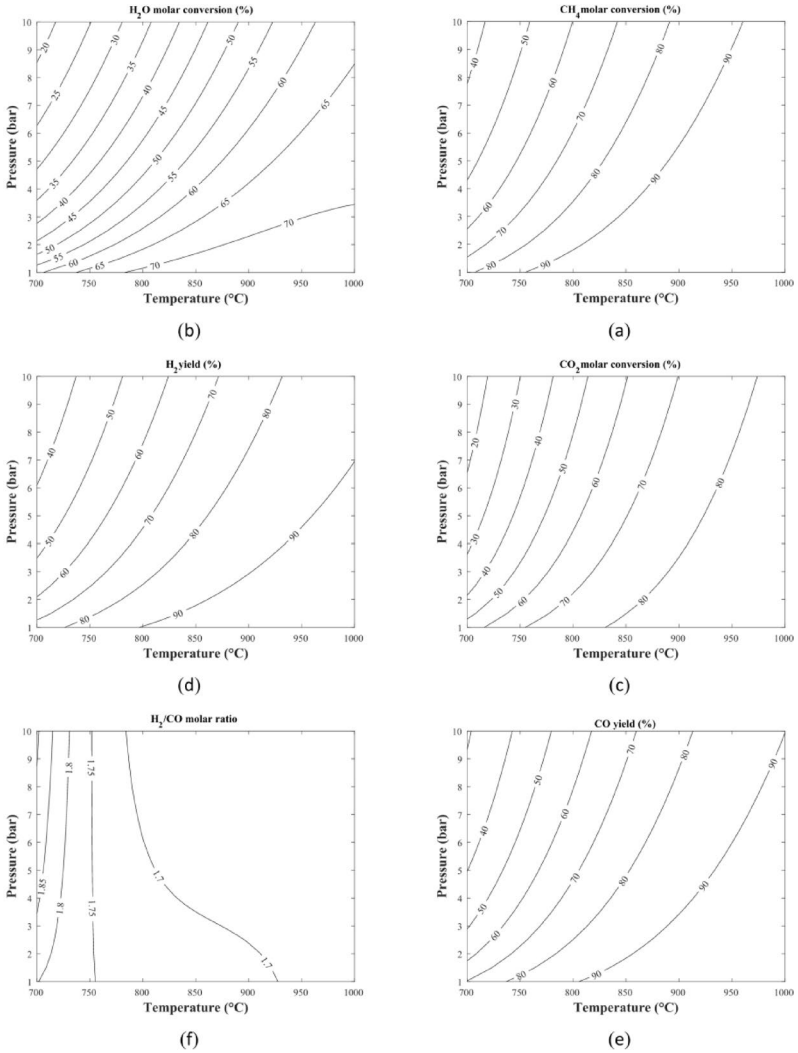

Fig. 5. Variations of the **(a)** CH_4, **(b)** H_2O, **(c)** CO_2 equilibrium conversion; **(d)** H_2, **(e)** CO molar yield; and **(f)** H_2/CO equilibrium molar ratio as a function of temperature and pressure at a fixed molar feed ratio of CH_4:H_2O: CO_2:O_2 = 1:0.54:0.48:0.1.

In addition, the very high pressures typically accelerate coke formation, but elevated pressures are often preferred to reduce the sizing of downstream compression stages for methanol or Fischer-Tropsch synthesis. So, it is necessary to maintain a careful balance between conversion, efficiency, and catalyst longevity[27].

Investigation of the effect of H_2O/CH_4 ratio in the feed

Figure 6 illustrates the influence of the H_2O/CH_4 ratio in the feed on reactant conversion, product yields, and the H_2/CO ratio in the outlet syngas.

As observed in Fig. 6a, the CH_4 conversion increases with a higher H_2O/CH_4 ratio. According to Le Chatelier's principle, increasing the H_2O concentration shifts the equilibrium of the SMR reaction toward the products (to the right), thereby enhancing the equilibrium conversion of CH_4. Furthermore, the additional H_2O inhibits carbon formation (coking) via CH_4 decomposition, which helps maintain catalyst activity for a longer duration and consequently improves CH_4 conversion.

Figure 6b illustrates that at lower temperatures, an increase in H_2O results in higher H_2O conversion. This is due to the shift in equilibrium of both the SMR and WGS reactions toward the products as the H_2O concentration increases. Conversely, at higher temperatures, the H_2O equilibrium conversion decreases as the concentration of H_2O increases. This occurs because, at elevated temperatures, the rate of CH_4-consuming reactions is high, making CH_4 the limiting reactant. H_2O consumption is thus constrained by its reaction capacity with the available CH_4, resulting in a significant portion of the H_2O leaving the reactor unreacted. It is important to note that this decrease in H_2O conversion does not imply lower energy efficiency, as the excess H_2O prevents coking and promotes H_2 production.

According to Fig. 6c, the CO_2 equilibrium conversion decreases with an increasing H_2O/CH_4 ratio. This is attributed to two factors: firstly, increased H_2O concentration enhances the WGS reaction (according to Le

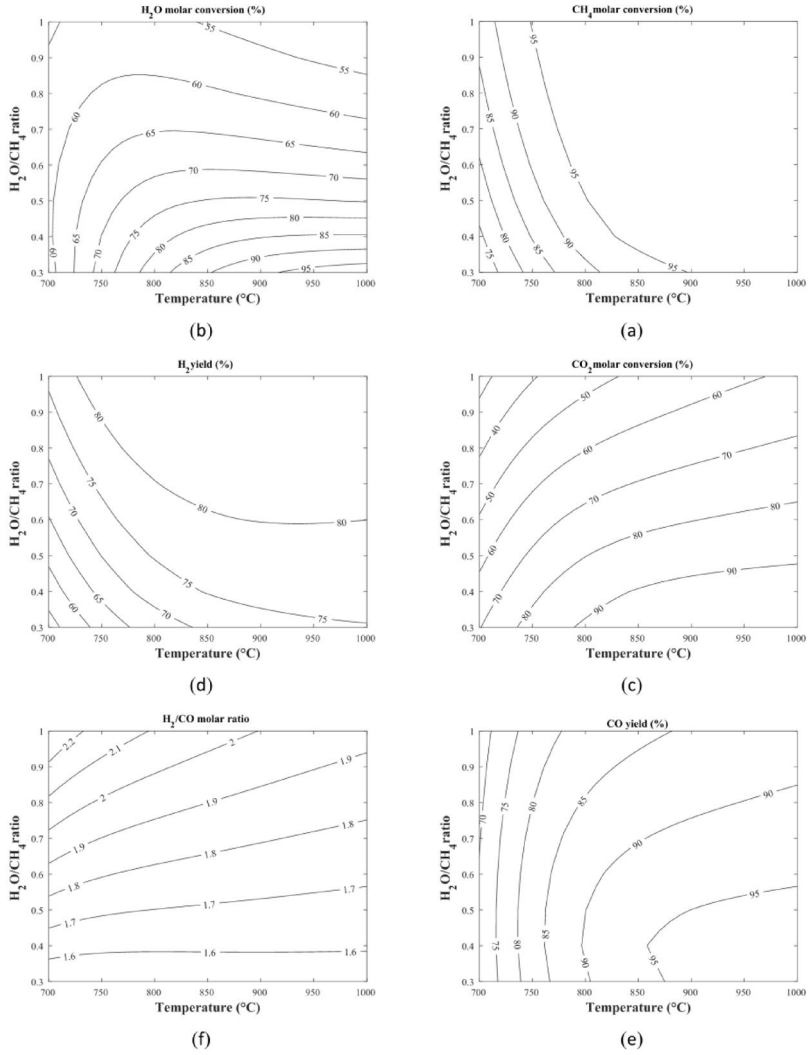

Fig. 6. Variations of the **(a)** CH_4, **(b)** H_2O, **(c)** CO_2 equilibrium conversion; **(d)** H_2, **(e)** CO molar yield; and **(f)** H_2/CO equilibrium molar ratio as a function of temperature and H_2O/CH_4 feed ratio at a fixed molar ratio of CH_4:CO_2:O_2 = 1:0.48:0.1 (with H_2O variable).

Chatelier's principle), leading to greater CO_2 production and thus a lower net conversion of CO_2. Secondly, in the context of combined reforming, CH_4 has a higher tendency to react with H_2O than with CO_2. Therefore, as the H_2O/CH_4 ratio increases, the SMR reaction is favored, leaving less CH_4 available for the DMR reaction, which further contributes to the reduced conversion of CO_2.

Figure 6d shows that increasing the H_2O/CH_4 ratio increases H_2 yield. As previously explained, this enhances both the SMR and WGS reactions, thereby increasing H_2 production. For CO, there are two competing effects: on the one hand, promoting SMR increases CO production, while on the other hand, enhancing the WGS reaction consumes CO, reducing the CO yield, as depicted in Fig. 6e.

Finally, Fig. 6f confirms that the H_2/CO ratio increases with the H_2O/CH_4 ratio, which is consistent with the discussed phenomena.

Investigation of the effect of CO_2/CH_4 ratio in the feed

The effect of the CO_2/CH_4 ratio in the feed on the CH_4, CO_2, and H_2O conversion, as well as on the H_2 and CO yield, and the H_2/CO ratio at various temperatures is presented in Fig. 7.

As observed, increasing the CO_2/CH_4 ratio enhances the equilibrium CH_4 conversion (Fig. 7a). This is attributed to the promotion of the DMR reaction with higher CO_2 concentrations. Conversely, increasing the CO_2 ratio has an inverse effect on H_2O conversion (Fig. 7b), as it promotes the RWGS reaction, which consumes H_2 and produces H_2O. Furthermore, and as expected, increasing the CO_2 concentration has a direct positive effect on its own conversion (Fig. 7c). According to Le Chatelier's principle, this increase shifts the equilibrium of the DMR reaction toward the products (right) and the WGS reaction toward the reactants (left), thereby increasing the equilibrium conversion of CO_2. It is important to note, however, that excessive CO_2—unlike H_2O—can lead to catalyst deactivation in the process.

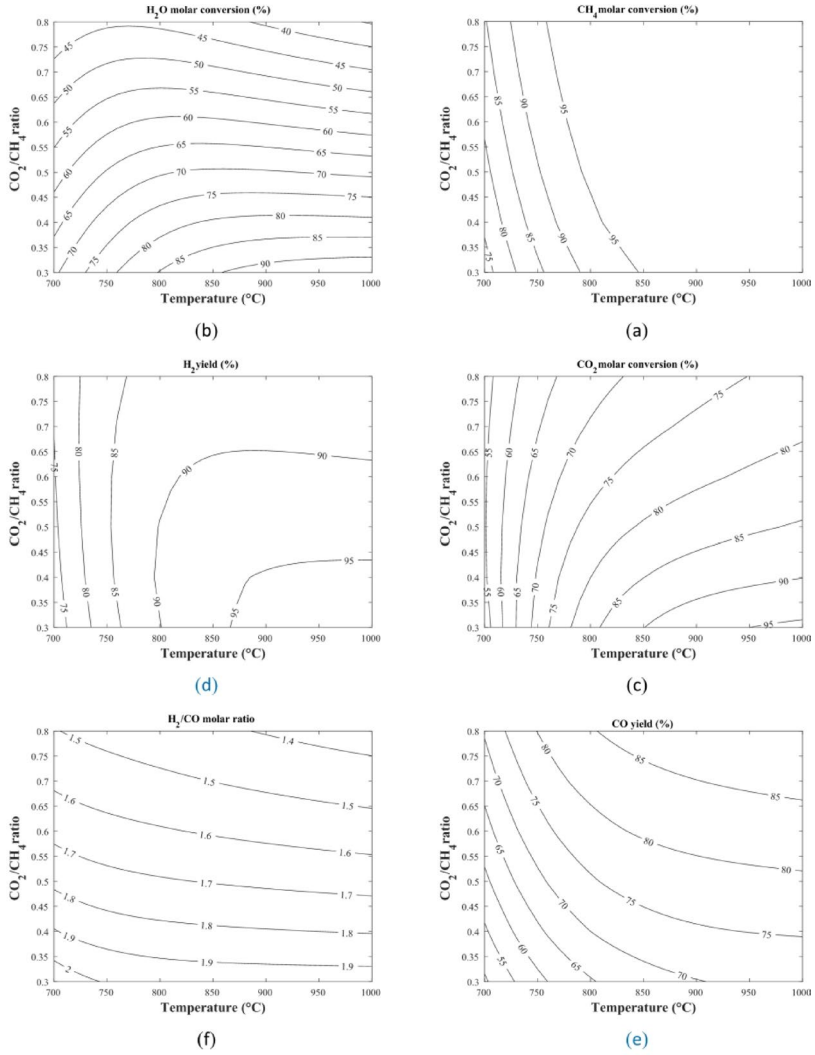

Fig. 7. Variations of the **(a)** CH_4, **(b)** H_2O, **(c)** CO_2 equilibrium conversion; **(d)** H_2, **(e)** CO molar yield; and **(f)** H_2/CO equilibrium molar ratio as a function of temperature and CO_2/CH_4 feed ratio at a fixed molar ratio of CH_4:H_2O: O_2 = 1:0.54:0.1 (with CO_2 variable).

Additionally, an increase in the CO_2/CH_4 ratio results in a higher CO molar yield (Fig. 7e). This occurs because the elevated CO_2 concentration further promotes the DMR and RWGS reactions, resulting in increased CO production.

Regarding the H_2 yield (Fig. 7d), it exhibits a temperature-dependent response to the CO_2/CH_4 ratio. At lower temperatures, increasing the CO_2/CH_4 ratio leads to a slight increase in H_2 yield. This is because the additional CO_2 promotes the DMR, which serves as a source of H_2 production. At these thermal conditions, the hydrogen generation from DMR outweighs its consumption via the RWGS reaction. However, as the temperature increases, the trend reverses, and the H_2 yield decreases with a higher CO_2/CH_4 ratio. In this high-temperature regime, the RWGS reaction becomes thermodynamically much more favorable and faster. Consequently, a significant portion of the H_2 produced by the reforming reactions is consumed by the excess CO_2 to form CO and H_2O.

As shown in Fig. 7e, the CO molar yield exhibits a monotonic increase with the CO_2/CH_4 ratio across all temperatures, driven by the synergistic promotion of both DMR and RWGS reactions. These combined effects explain the significant reduction in the equilibrium H_2/CO ratio as the feed becomes richer in CO_2 (Fig. 7f), highlighting the necessity of balancing CO_2 levels to maintain the desired syngas quality for downstream synthesis.

Investigation of the effect of O_2/CH_4 ratio in the feed

Figure 8 illustrates the influence of the O_2/CH4 ratio in the feed on reactant conversion, product yields, and the H_2/CO ratio in the produced syngas.

As shown in Fig. 8a and c, increasing the oxygen concentration leads to an increase in the equilibrium CH_4 conversion, while the H_2O and CO_2 equilibrium conversions decrease. This behavior occurs because a higher oxygen concentration promotes CH_4 consumption via both POX and full combustion reactions, thereby reducing

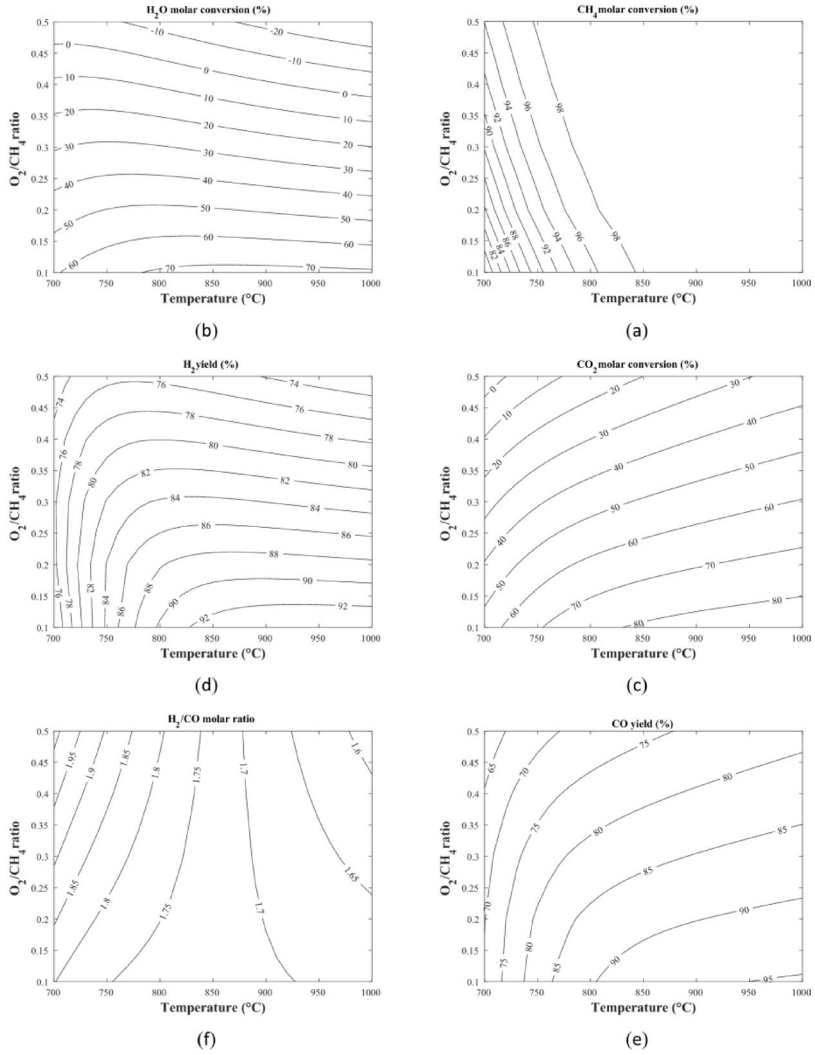

Fig. 8. Variations of the **(a)** CH_4, **(b)** H_2O, **(c)** CO_2 equilibrium conversion; **(d)** H_2, **(e)** CO molar yield; and **(f)** H_2/CO equilibrium molar ratio as a function of temperature and O_2/CH_4 feed ratio at a fixed molar ratio of CH_4:CO_2:O_2 = 1:0.54:0.48 (with O_2 variable).

the extent of CH_4 reforming (dry and steam). Additionally, the complete combustion of CH_4 produces CO_2 and H_2O, thereby lowering the net equilibrium conversion of these components. Also, as discussed, increasing the oxygen concentration decreases the molar yields of H_2 and CO, as demonstrated in Fig. 8d and e.

The H_2/CO molar ratio exhibits a complex temperature-dependent behavior with respect to oxygen concentration, as depicted in Fig. 8f. At lower temperatures (typically below 800 °C), increasing the O_2/CH_4 ratio leads to a higher H_2/CO ratio. This is primarily due to the dominance of full combustion and the subsequent WGS reaction, where the generated H_2O promotes H_2 production. However, a significant reversal in this trend is observed at higher temperatures (above 900 °C). In this elevated thermal regime, increasing oxygen concentration causes a decline in the H_2/CO ratio. This reversal occurs because high temperatures favor the POX of methane and the endothermic RWGS reaction, both of which significantly enhance the thermodynamic stability and production rate of CO relative to H_2. Therefore, the impact of oxygen on syngas quality is not uniform; it acts as a promoter for the H_2/CO ratio at low temperatures but shifts toward CO enrichment at high temperatures, necessitating careful thermal management to achieve the stoichiometric requirements for methanol synthesis.

Optimization results

This section presents the optimal operating conditions for achieving syngas with an H_2/CO ratio of 2, which is suitable for methanol production. The investigated operating parameters included temperature (700–1000 °C), pressure (1–10 bar), H_2O/CH_4 ratio (0.3–1), CO_2/CH_4 ratio (0.3–0.8), and O_2/CH_4 ratio (0.1–0.5).

The objective function for the optimization was defined by Eq. (20), which was minimized during the process:

$$FitnessFunction = \left| 2 - \frac{molesof H_2 produced}{molesof COproduced} \right| \tag{20}$$

Parameter	Value
Temperature (°C)	989
Pressure (bar)	1.0
H_2O/CH_4 ratio	0.61
CO_2/CH_4 ratio	0.30
O_2/CH_4 ratio	0.10

Table 3. Optimal operating conditions for producing syngas suitable for methanol synthesis.

In addition to the H_2/CO ratio in the produced syngas, the conversion percentages of CH_4 and CO_2 were also considered critical. Therefore, the optimization problem was subject to two constraints: CH_4 and CO_2 conversion must both exceed 90%. Thus, the problem was formulated as a single-objective optimization with inequality constraints.

Table 3 summarizes the optimal operating conditions derived from the optimization. The optimization results demonstrate that to satisfy the dual requirement of high CO_2 conversion (90%) and a precise H_2/CO ratio of 1.99, the system converges toward a low-pressure and high-temperature regime. Operating at 1.0 bar is essential to maximize the conversion of CO_2, as the DMR is a mole-increasing process. Furthermore, the identified temperature of 989 °C provides the necessary thermal energy to drive the endothermic reactions, compensating for the lower O_2/CH_4 and CO_2/CH_4 ratios required to meet the conversion constraints. While the current optimization focuses on syngas quality and conversion, the global energy balance is considered outside the scope of this study.

Conclusion

This study was conducted in two main parts. In the first part, a thermodynamic analysis of the TRM process was performed using MATLAB R2024b, which simultaneously solves a system of nonlinear equations that includes reaction equilibrium constants and mass balance equations. Accordingly, the equilibrium composition of various components was calculated under different operating conditions and feed ratios. Subsequently, the effects of parameters such as temperature, pressure, and the ratios of H_2O/CH_4, CO_2/CH_4, and O_2/CH_4 on the CH_4, CO_2, and H_2O conversion, as well as the H_2 and CO yields and their ratio in the produced syngas, were investigated.

The results indicate that increasing temperature significantly promotes CH_4 and CO_2 conversions and H_2 and CO yield; however, H_2O conversion exhibits a non-monotonic trend, characterized by an initial increase followed by a decline at elevated temperatures. The H_2/CO ratio decreases with increasing temperature because CO is more thermodynamically stable. Operating pressure has a dual impact. While it generally decreases reactants conversion, its effect on the H_2/CO ratio is strictly temperature-dependent, exhibiting an inversion behavior in which the pressure's influence reverses across different thermal regimes. Regarding feed ratios, H_2O/CH_4 increases H_2 yield and the H_2/CO ratio, whereas CO_2/CH4 favors CO production and reduces the H_2/CO ratio. The O_2/CH_4 ratio acts as a temperature-sensitive regulator, increasing the H_2/CO ratio below 800 °C but promoting CO enrichment above 900 °C.

The second part of this study focused on optimizing the operating conditions to produce syngas suitable for methanol production using a GA. A single-objective optimization problem with constraints was defined, aiming to minimize the absolute difference between the H_2/CO ratio and the target value of 2. The constraints required that the CH_4 and CO_2 conversion exceed 90% under optimal conditions.

The optimization results revealed that a high-temperature and low-pressure environment is essential to overcome thermodynamic limitations and achieve the stringent constraint of 90% CO_2 conversion. The optimal point was identified at a temperature of 989 °C and a pressure of 1.0 bar, with a feed composition of CH_4:H_2O:CO_2:O_2 = 1:0.61:0.30:0.10. Under these verified conditions, the CH_4 conversion exceeds 99% and the CO_2 conversion reaches the 90% threshold, yielding a syngas ratio of 1.99, which is ideal for industrial methanol synthesis.

These findings demonstrate that while tri-reforming of methane is a complex process influenced by competing reactions, a precise balance of feed ratios—particularly maintaining a lower O_2/CH_4 and CO_2/CH_4 ratio at atmospheric pressure—can maximize the conversion of greenhouse gases. The optimization data are fully consistent with the parametric sensitivity analysis, providing a reliable thermodynamic framework for the design and operation of TRM reactors. This study offers a clear roadmap for achieving high-purity syngas while optimizing the environmental benefits of CO_2 utilization in the petrochemical industry.

It should be noted that the optimization performed in this study is focused primarily on the thermodynamic equilibrium and the target syngas quality. While the identified optimal temperature (989 °C) ensures high CO_2 conversion, the optimization of the overall energy balance and thermal efficiency of the reactor is outside the scope of the present paper.

Data availability

The datasets used and analysed during the current study available from the corresponding author on reasonable request.

Received: 8 November 2025; Accepted: 11 March 2026

Published online: 19 March 2026

References

1. Ashour, A., Challiwala, M. S., Musa, T., Wilhite, B. & Elbashir, N. Modeling tri-reforming of methane for carbon dioxide utilization and hydrogen production.. *Energy* https://doi.org/10.1016/j.energy.2025.137977 (2025).
2. Alli, R. D., de Souza, P. A., Mohamedali, M., Virla, L. D. & Mahinpey, N. Tri-reforming of methane for syngas production using Ni catalysts: current status and future outlook. *Catal. Today*. **407**, 107–124 (2023).
3. Arab Aboosadi, Z., Farhadi, M. & Yadecoury Thermally intensification of steam reforming process by use of methane tri-reforming: a review. *Int. J. Chem. Reactor Eng.* **17** (12), 20190108 (2019).
4. Pham, X. H. et al. Review on the catalytic tri-reforming of methane-Part II: Catalyst development. *Appl. Catal. A.* **623**, 118286 (2021).
5. Minh, D. P., Pham, X. H., Siang, T. J. & Vo, D. V. N. Review on the catalytic tri-reforming of methane-Part I: Impact of operating conditions, catalyst deactivation and regeneration. *Appl. Catal. A.* **621**, 118202 (2021).
6. Gupta, S. & Deo, G. Effect of metal amount on the catalytic performance of Ni–Al2O3 catalyst for the tri-reforming of methane. *Int. J. Hydrog. Energy* **48**(14), 5478–5492 (2023).
7. Kumar, R., Kumar, K., Pant, K. & Choudary, N. Tuning the metal-support interaction of methane tri-reforming catalysts for industrial flue gas utilization. *Int. J. Hydrog. Energy*. **45** (3), 1911–1929 (2020).
8. Osat, M., Shojaati, F. & Hafizi, A. A multi-objective optimization of three conflicting criteria in a methane tri-reforming reactor. *Int. J. Hydrog. Energy*. **48** (16), 6275–6287 (2023).
9. Alipour-Dehkordi, A. & Khademi, M. H. O2, H2O or CO2 side-feeding policy in methane tri-reforming reactor: The role of influencing parameters. *Int. J. Hydrog. Energy*. **45** (30), 15239–15253 (2020).
10. Sharma, A., Terefe, R. & Biswas, P. Optimization of reaction parameters by response surface methodology for the tri-reforming process over a Ni-silica catalyst to produce synthesis gas. *Int. J. Hydrog. Energy*. **156**, 150378 (2025).
11. Rouhandeh, H. & Behroozsarand, A. Simulation and optimization of methanol production process via bi-reforming of methane: A novel genetic algorithm-based approach in Python. *Int. J. Hydrogen Energy* **101**, 1161–1171 (2025).
12. Rajabi, R. F., Rezaei, E. & Kozinski, J. Comparative minimization of CO2 emissions of methanol synthesis via tri-reforming and gas-heated reforming of methane. *Int. J. Hydrog. Energy*. **152**, 150185 (2025).
13. Boakye, O. Y., Hashemi, S. M. & Mahinpey, N. Investigation of Al2O3, ZrO2, SiO2, and CeO2 supported nickel catalysts for tri-reforming of methane. *Int. J. Hydrogen Energy* **109**, 802–812 (2025).
14. Niska, V. M. et al. Biogas Bi-and Tri-reforming over Ni/Al2O3 and Ni/ZrO2–Effect of the reaction conditions on conversions, carbon formation, and biohydrogen-carbon monoxide ratio. *Int. J. Hydrog. Energy*. **162**, 150684 (2025).
15. Sharma, A. & Biswas, P. Methane tri-reforming over Ni, Ru monometallic and Ni-Ru bimetallic catalyst supported on MIL-53 metal-organic framework. *Catal. Today*. **450**, 115209 (2025).
16. de Souza, P. A., Afzal, R. M., Camacho, F. G. & Mahinpey, N. Catalyst development for the tri-reforming of methane (TRM) process by integrated singular machine learning models. *Can. J. Chem. Eng.* **103** (2), 758–770 (2025).
17. Zhang, Y., Zhang, S., Gossage, J. L., Lou, H. H. & Benson, T. J. Thermodynamic analyses of tri-reforming reactions to produce syngas. *Energy Fuels* **28**(4), 2717–2726 (2014).
18. Szczygieł, J. et al. Thermodynamical analysis and optimization of dry reforming and trireforming of greenhouse gases: A statistical approach.. *ACS. Omega* https://doi.org/10.1021/acsomega.5c03980 (2025).
19. Chein, R. Y. & Hsu, W. H. Thermodynamic analysis of syngas production via tri-reforming of methane and carbon gasification using flue gas from coal-fired power plants. *J. Clean. Prod.* **200**, 242–258 (2018).
20. Jarungthammachote, S. *Optimum feed ratio analysis for tri-reforming of methane using thermodynamic equilibrium method* p. 68–79 (Science & Technology Asia, 2015).
21. Okonkwo, O., Yablonsky, G. & Biswas, P. Thermodynamic analysis of tri-reforming of oxy-fuel combustion exhaust gas. *J. CO2 Utilization*. **39**, 101156 (2020).
22. Farsi, M. & Lari, M. F. Methanol production based on methane tri-reforming: Process modeling and optimization. *Process Saf. Environ. Prot.* **138**, 269–278 (2020).
23. Lim, D., Lee, B., Lee, H., Byun, M. & Lim, H. Projected cost analysis of hybrid methanol production from tri-reforming of methane integrated with various water electrolysis systems: Technical and economic assessment. *Renew. Sustain. Energy Rev.* **155**, 111876 (2022).
24. Soleimani, S. & Lehner, M. Tri-reforming of methane: thermodynamics, operating conditions, reactor technology and efficiency evaluation—a review. *Energies* **15** (19), 7159 (2022).
25. Farsi, M., Lari, M. F. & Rahimpour, M. Development of a green process for DME production based on the methane tri-reforming. *J. Taiwan Inst. Chem. Eng.* **106**, 9–19 (2020).
26. Challiwala, M., Ghouri, M., Linke, P., El-Halwagi, M. & Elbashir, N. A combined thermo-kinetic analysis of various methane reforming technologies: Comparison with dry reforming. *J. CO2 Util.* **17**, 99–111 (2017).
27. Song, C. & Pan, W. Tri-reforming of methane: A novel concept for catalytic production of industrially useful synthesis gas with desired H_2/CO ratios. *Catal. Today* **98**(4), 463–484 (2004).
28. Kozonoe, C. E., Alves, R. M. B. & Schmal, M. Influence of feed rate and testing variables for low-temperature tri-reforming of methane on the Ni@ MWCNT/Ce catalyst. *Fuel* **281**, 118749 (2020).
29. De Oliveira, M. J. *Equilibrium thermodynamics* (Springer, 2013).
30. Rossi, C., Cardozo-Filho, L. & Guirardello, R. Gibbs free energy minimization for the calculation of chemical and phase equilibrium using linear programming. *Fluid Phase Equilib.* **278**(1–2), 117–128 (2009).
31. Néron, A., Lantagne, G. & Marcos, B. Computation of complex and constrained equilibria by minimization of the Gibbs free energy. *Chem. Eng. Sci.* **82**, 260–271 (2012).
32. Jafarbegloo, M., Tarlani, A., Mesbah, A. W. & Sahebdelfar, S. Thermodynamic analysis of carbon dioxide reforming of methane and its practical relevance. *Int. J. Hydrog. Energy*. **40** (6), 2445–2451 (2015).
33. Azarhoosh, M. J., Halladj, R. & Askari, S. Application of evolutionary algorithms for modelling and optimisation of ultrasound-related parameters on synthesised SAPO-34 catalysts: crystallinity and particle size. *Prog. React. Kinet. Mech.* **43** (3–4), 236–243 (2018).
34. Alotaibi, F. N., Berrouk, A. S. & Saeed, M. Optimization of yield and conversion rates in methane dry reforming using artificial neural networks and the multiobjective genetic algorithm. *Ind. Eng. Chem. Res.* **62** (42), 17084–17099 (2023).
35. Azarhoosh, M., Farivar, F. & Ebrahim, H. A. Simulation and optimization of a horizontal ammonia synthesis reactor using genetic algorithm. *RSC Adv.* **4** (26), 13419–13429 (2014).
36. Yu, X. et al. Multi-objective optimization of ANN-based PSA model for hydrogen purification from steam-methane reforming gas. *Int. J. Hydrog. Energy*. **46** (21), 11740–11755 (2021).
37. Lotfi, N., Ebrahim, H. A. & Azarhoosh, M. J. Proposing a novel theoretical optimized model for the combined dry and steam reforming of methane in the packed-bed reactors. *Chem. Pap.* **73** (9), 2309–2328 (2019).

Author contributions

Amin Alamdari: Writing – review & editing, Conceptualization. M.J. Azarhoosh: Methodology, Formal analysis, Validation, Software, Writing – original draft. A. Aghaeinejad-Meybodi: Writing – review & editing.

Declarations

Competing interests

The authors declare no competing interests.

Additional information

Correspondence and requests for materials should be addressed to A.A. or M.J.A.

Reprints and permissions information is available at www.nature.com/reprints.

Publisher's note Springer Nature remains neutral with regard to jurisdictional claims in published maps and institutional affiliations.